Predicting the hydrological response of a forest after wildfire and soil treatments using an Artificial Neural Network

Predicting the hydrological response of a forest after wildfire and soil treatments using an Artificial Neural Network

Demetrio Antonio Zema[1,*], Manuel Esteban Lucas-Borja[2], Lidia Fotia[3], Domenico Rosaci[4], Giuseppe M. L. Sarnè[3], Santo Marcello Zimbone[1]

[1] *Department AGRARIA, University "Mediterranea" of Reggio Calabria, Località Feo di Vito, I-89122 Reggio Calabria (Italy)*

[2] *Departamento de Ciencia y Tecnología Agroforestal y Genética, Universidad de Castilla La Mancha, Campus Universitario s/n, C.P. 02071, Albacete (Spain)*

[3] *Department DICEAM, University "Mediterranea" of Reggio Calabria, Località Feo di Vito, I-89122 Reggio Calabria (Italy)*

[4] *Department DIIES, University "Mediterranea" of Reggio Calabria, Località Feo di Vito, I-89122 Reggio Calabria (Italy)*

* corresponding author, dzema@unirc.it

ABSTRACT

Accurate predictions of surface runoff and soil erosion after wildfire help land managers adopt the most suitable actions to mitigate post-fire land degradation and rehabilitation planning. The use of the Artificial Neural Networks (ANNs) is advisable as hydrological prediction tool, given their lower requirement of input information compared to the traditional hydrological models.

This study proposes an ANN model, purposely prepared for forest areas of the semi-arid Mediterranean environments. The ANN hydrological prediction capability in non-burned, burned by wildfire, and burned and then treated soils has been verified at the plot scale in pine forests of

South-Eastern Spain. Runoff and soil loss were much higher than non-burned soils (assumed as control), but mulch application was effective to control runoff and soil erosion in burned plots. Moreover, logging did not affect the hydrological response of these soils. The model gave very accurate runoff and erosion predictions in burned and non-burned soils as well as for all soil treatments (mulching and/or logging or not), with only one exception (that is, in the condition with the combination of treatments which gave the worst performance, burning, mulching and logging), as shown by the exceptionally high model efficiency and coefficients of determination. Although further experimental tests are needed to validate the ANN applicability to the burned forests of the semi-arid conditions and other ecosystems, the use of ANN can be suggested to landscape planners as decision support system for the integrated assessment and management of forests.

KEYWORDS: Artificial Intelligence; hydrological modelling; surface runoff; erosion; mulching; logging.

1. INTRODUCTION

The increased frequency and severity of summer droughts due to the forecasted global warming are expected to lead to an important increase in the severity and recurrence of wildfires, which may affect processes and properties of forest soils (Certini, 2014). Forest fire generates a chain of physico-chemical and biological processes, whose effects influence the entire ecosystem. One of the most threatening effect of forest fire soil is the change in its post-fire hydrological response, strictly linked to fire severity (Morales et al., 2000; Benavides-Solorio and MacDonald, 2005; Robichaud et al., 2007). In other words, the more severe the fire is, the greater is the susceptibility to surface runoff and soil erosion. More specifically, key factors enhancing runoff and soil loss are the reduction in infiltration, increase in water repellence, destruction of vegetal cover, and loss of soil organic matter (Larsen et al., 2009; Neary et al., 2005). The changes in soil hydrology induced by

wildfire are of high importance particularly in Mediterranean areas, where the infiltration-excess mechanism dominates runoff and erosion generation (Plaza-Alvarez et al., 2019). In such an environmental context, intense storm events in autumn and hot summers with drought risks make these zones prone to post-fire erosion and wildfire occurrence, respectively (Shakesby, 2011). Therefore, the post-fire changes in soil hydrology are the key to understand the post-fire restoration; however, the number of the studies analysing the post-fire effects on soils at multi-year scale is larger than short-term research (few months after fire).

Moreover, it is very important to understand the hydrological effects (that is, the potential reduction of surface runoff and erosion) of the post-fire stabilization and rehabilitation treatments, used to mitigate the short-term effects on soil degradation (Robichaud et al., 2000). Among these treatments, emergency post-fire activities for soil stabilization, such as mulching, are recommended in areas burned by wildfire to minimize overland flow and erosion risk (Vega et al., 2014). In any case, the need of a better understanding and prediction of the hydrological effects of wildfire fires has created a strong demand for tool able to simulate post-fire runoff and soil loss (Moody et al., 2013). Accurate predictions of water and sediment flows after fire help land managers in the adoption of the most suitable actions to mitigate post-fire land degradation and rehabilitation planning (Moody et al., 2013). With regards to post-fire erosion modelling, literature reports simple empirical models (such as the Universal Soil Loss Equation, USLE, and its revised version, the RUSLE model), semi-empirical models (e.g., the revised Morgan–Morgan–Finney model, Morgan 2001), and physically-based models (for instance, the Water Erosion Prediction Project (WEPP). However, many hydrological models were developed for agricultural regions, and thus such models may find limited applicability in burned conditions of the Mediterranean ecosystems (Esteves et al., 2012; Vieira et al., 2014; 2018).

In the last two decades data-driven models, such as the Artificial Neural Networks (ANNs), had an increasing popularity for estimating and forecasting water resources (Hsu et al., 1995; Riad et al., 2004; Sharma and Tiwari, 2009). The ANNs have been applied to complex, dynamic and highly

93 non-linear systems (Hsu et al., 1995), and in situations where the input is incomplete or ambiguous,
94 since they can analyze multi-source dataset (Tokar and Johnson, 1999). The main advantage of the
95 ANNs over traditional methods is the lower requirements of information about the complex nature
96 of the underlying process that are instead described in a mathematical closed form (Sudheer et al.,
97 2002). Furthermore, ANNs can generalise relationships also from a small dataset, but remain more
98 or less robust when noisy or missing inputs are present and can work also in changing environments
99 (Dawson and Wilby, 1998). ANNs learn from the analysis of the available input data and do not
100 require reprogramming, but they must be trained, optimized and tested (Gholam et al., 2018).
101 ANNs have been extensively used also for rainfall-runoff modeling, flood predictions, reservoir
102 operations, routing of polluting compounds (ASCE, 2000). For instance, ANNs have been used for
103 modelling the rainfall-runoff relationships in small to large watersheds of United States (Hsu et al.,
104 1995), United Kingdom (Dawson and Wilby, 1998), India (Sudheer et al., 2002; Sharma and
105 Tiwari, 2009), Morocco (Riad et al., 2004), Albaradeya et al., 2011 (in Palestinian territories) and,
106 more recently, in Australia (Asadi et al., 2019). Also, soil erosion was predicted using ANNs at
107 both plot scale (Licznar and Nearing, 2003, and Kim and Gilley, 2008, in USA; Albaradeya et al.,
108 2011, in Palestinian territories) and watershed scale (e.g., Gholami et al., 2018, in Iran). Moreover,
109 Yusof et al. (2014) used ANNs to predict the soil erodibility factor of the USLE equation using 74
110 samples of Malaysia soils.
111 However, only a few studies have analysed the ANN performance in soil erosion modelling
112 (Gholami et al., 2018) and, even, ANN has not been used for hydrological predictions in burned
113 soils. Modelling soil erosion and runoff after wildfires using ANNs may be a novel approach that
114 could be of help to better understand and predict fire-induced effects after fire.
115 To fill this gap, this study provides an ANN model, purposely prepared for pine forest areas of the
116 semi-arid Mediterranean environments, and verifies its hydrological prediction capability in non-
117 burned, burned by wildfire, and burned and then treated soils. More specifically, surface runoff and
118 soil loss were firstly measured in *i*) unburned plots (assumed as control); *ii*) plots subjected to a

wildfire and not rehabilitated with any post-fire measures; *iii*) plots subjected to fire and treated with mulching throughout one year. Based on these observations, the ANN model is calibrated and its performance in estimating surface runoff and soil loss at the event scale is evaluated under the peculiar climatic conditions and forest management.

2. MATERIALS AND METHODS

2.1. Experimental site and design

2.1.1. Study area

The study was carried out in the Sierra de las Quebradas forest (Liétor, Castilla-La Mancha region, province of Albacete, Central Spain) (Figure 1a). The climate is hot dry Mediterranean (Allué, 1990), *BSk* according to the Koppen classification (Kottek et al., 2006). Average annual rainfall and medium annual temperature is 282 mm and 16 °C, respectively. Elevation ranges between 520 and 770 m and aspect is W-SW. According to the Spanish Soil Map (2000), soils are classified as *Inceptisols* and *Aridisols* and soil texture is sandy loam.

The forest land mainly consists of *Pinus halepensis* M. stands. The mean density and height of forest trees before the wildfire were about 500–650 trees/ha and 7–14 m, respectively. The shrubs and herbaceous species mainly found at the study site were *Rosmarinus officinalis* L., *Brachypodium retusum* (Pers.) Beauv., *Cistus clusii* Dunal, *Lavandula latifolia* Medik., *Thymus vulgaris* L., *Helichrysum stoechas* (L.), *Stipa tenacissima* (L.), *Quercus coccifera* L. and *Plantago albicans* L.

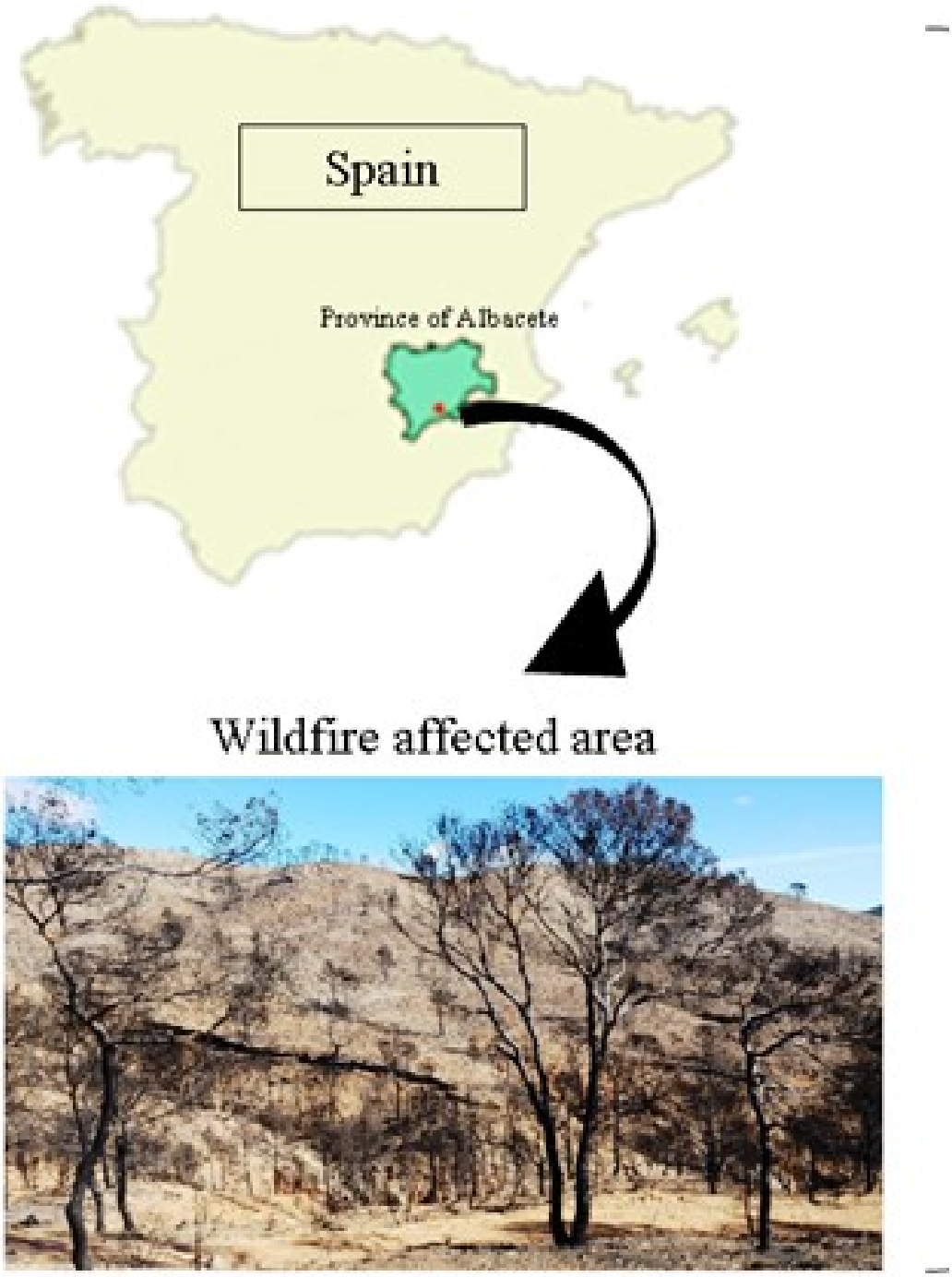

143

144

145 Figure 1 - Location/experimental design (a) and measuring equipment (b) of the experimental plots

146 used to model the hydrological response of pine forest to wildfire using ANNs (Liétor, Castilla La

147 Mancha, Spain).

148

149 *2.1.2. Experimental site description*

150

151 Immediately after the wildfire, one site of about five hectares in the forest stand was selected for
152 study (Figure 1a). Twelve experimental plots (each one 9 m long and 3 m wide, for a total area of
153 27 m^2) were installed with their longest dimension along the maximum slope in the burned area. In
154 addition, an unburned area, located 7 km far from the burned stand was selected as control and three
155 other plots were located for the same aim.
156 In both areas, the plots were distributed caring that their characteristics (soil properties, slope and
157 aspect) were similar, to ensure comparability. Plot slope varied between 10 and 15%. Plot distance
158 was always higher than 20 m.
159 The plots, delimitated by a 0.5 m wide geotextile fabric that was inserted up to 0.4 m below the
160 ground surface, were hydraulically isolated along their perimeter to prevent external inputs of water
161 and sediments. For this, a geotextile that was tightly fastened to 0.8 m long and 20 mm in diameter
162 iron rods was pounded into the ground at 0.15 m of depth. A 50 cm long metallic sediment fence
163 with a triangular shape was installed in the downstream side of the plot, to convey water and
164 sediments in a pipe and then into a 25 litre tank. The area with the metallic fence was protected
165 from rain by a plastic cover. Its ground surface was also covered by plastic, to ensure that the entire
166 runoff and all sediments were delivered to the collection point and then to the storage container
167 (Figure 1b).

168

169 *2.1.3. Wildfire and forest management operations*

170

171 The Sierra de las Quebradas area was affected in July 2016 by a wildfire. During the wildfire about
172 830 ha of forest land was burned. Tree mortality was 100%. A mean value of soil burn severity was
173 obtained for each plot by adopting the methodology proposed by Vega et al. (2013) and Fernandez

et al. (2017). Soil burn severity values were classified in the high class for all of the burned plots by the Castilla La Mancha Forest Service.

In September 2016, mulching treatment was carried out in six plots in the burned area. Mulching consisted of manually spreading straw of barley on the plots at a rate of 200 g/m^2 (dry weight). Initial mulch cover and depth were 95% of the plot area and 3 cm, respectively.

Moreover, salvage logging was conducted in December 2016 in six plots, of which three non-mulched and three mulched. The geotextile fabrics of the plots were removed before harvesting and re-installed immediately after. The trees were cut with mechanical chain saws and burned logs were removed using an agricultural tractor equipped with pneumatic wheels.

The experimental design consisted of the following *soil conditions* in relation to the wildfire: (1) "*Non-Burned, NB"* (three plots); (2) "*Burned, B*" (twelve plots). After fire the following *soil treatments* were defined in the burned plots: (i) *Burned+Mulching+No-Logging (B+M+NL,* six plots*)*; (ii) *Burned+No-Mulching+No-Logging (B+NM+NL,* six plots*).* This experimental design was adjusted from the cutting date onwards, and the treatments were reassigned as follows: *i*) *Burned+Mulching+Logging* (*B+M+L*, three plots); *ii*) *Burned-No-Mulching+Logging* (*B+NM+L*, three plots).

2.1.4 Collection of observed data

Precipitation depth, duration and intensity were measured by a weather station (WatchDog 2000 Series model) with a tipping bucket rain gauge, located 50 m out of the study area. In the hourly rainfall series of the experimental database, two consecutive events were considered separate, if no rainfall was recorded for 6 h or more (Wischmeier and Smith, 1978; Zema et al., 2017).

Between September 2016 and July 2017, after each precipitation event, the volume of surface runoff collected by the plot tank was measured. After mixing the runoff water collected in the tank, a water sample of about 0.5 litres was collected. Then, samples were oven dried (at 105 °C) for 24 h

in the laboratory and Total Dissolved Sediments (TDS) and Suspended Sediments (SS) were measured. Moreover, the eroded soil deposited at each metallic sediment fence was collected manually after each event and then weighed in the field. After sample oven-drying, the dry sediment (DS) weight was measured.

The runoff coefficients of each event were calculated as the ratio surface runoff to total rainfall. Soil loss was evaluated as the sum of DS, TDS and SS.

2.1.5 Statistical analysis on observed data

Following Lucas-Borja et al. (2019), the observed data were analysed to evaluate the treatment effect (with five levels: *Non-Burned, Burned+No-Mulching+No-Logging, Burned+Mulching+No-Logging, Burned+No-Mulching+Logging Burned+No-Mulching+No-Logging*) on runoff volumes and soil losses by a general linear mixed model. The survey date and plots were included as random effects. The rainfall parameters (total precipitation, maximum rainfall intensity in 60 min of each rainy event) for each sediment collection date were included as covariates. Data were log-transformed to achieve normality and residuals were tested for autocorrelation, normality and homogeneity of variance. When significant mixed effects were indicated, the post hoc pairwise comparisons (with Bonferroni adjustment for multiple comparisons) were conducted to assess differences between the main effects of treatments and their interactions. All the statistical analyses were conducted using the R statistical program, package lme4.

2.2. Implementation of the Artificial Neural Networks

2.2.1. Theoretical approach about the Artificial Neural Networks

In this work a standard feedforward neural network has been used to simulate the hydrological response of the experimental plots. A standard feedforward neural network (Haykin, 1994) is composed by a set of N nodes *N* and a set of M arcs *A* (see Figure 2). The nodes are partitioned into L groups, called *layers*, with L > 2. The first layer is a set of *I* input nodes *NI* called *input layer*; then, there are L-2 *hidden layers*, of which each hidden layer h_t, with t = 1, .., L-2 is a set of *H* nodes NH_t. Finally, there is a set of *O* nodes *NO*, called *output layer*. Each node (denoted by *o*) of the output layer is connected with each node (denoted by *h*) of the NH_{L-2} hidden layer by an edge directed from *o* to *h*, and each node *y* of the NH_1 hidden layer is connected by an edge with each node *x* of the input layer by an edge directed from *y* to *x* .

For each edge of the network, we denote by *i* (resp. *j*) the source (resp. destination) node and we associate a real value W_{ij}, called *weight*, with the edge.

The neural network is used for representing a real function. Each input layer node is associated with an input (real) value and each output layer node is associated with an output (real) value of the function. The output values are computed by the neural network using the input values. Hidden layer nodes are associated with intermediate results of the computation.

The neural network computes the output values as follows. Both of each hidden and output layer node *n* are provided with the same function *a*, which is called *activation function*, and with a parameter Θ, which is called *bias*. The node *j* of the first hidden node NH_1 computes its associated hidden value $h_1 = a\left(\sum_{i=1}^{I} W_{ij} * I_i - \Theta\right)$, where *i* is an input layer node, i.e., by computing the weighted sum of the values I_i of the input layer using the weights W_{ij} associated with all the connections between each input layer node *i* and the hidden layer node *j*.

The node *j* of each hidden layer NH_l computes its associated hidden value $h_j^l = a\left(\sum_{i=1}^{H} W_{ij} * h_i^{l-1} - \Theta\right)$, where *i* is the l-1 layer node, i.e., by computing the weighted sum of the

values h_i^{l-1} of the nodes of the previous layer. Analogously, each output layer node j computes its associated output value $o_j = a\left(\sum_{i=1}^{H} W_{ij} * h_i^{L-2} - \Theta\right)$, where h_i^{L-2} is a hidden L-2 layer node.

The weight W_{ij} associated with the edges of the set A and the activation function parameters are suitably set by a *training algorithm* that tries to learn how correctly approximating the desired output. Training algorithms can be unsupervised or supervised. In the first case, the ANN autonomously learns the functional dependence between an input and its correct output. Differently, a supervised training algorithm takes advantage from the availability of a training dataset where for each input its correct output is provided; by measuring the difference between the correct and the computed ANN outputs then it is possible to tune the ANN parameters to minimize this error. When the ANN reaches the desired precision in reproducing the outputs of the training dataset, then the learnt ends and the ANN can be considered ready to work with unknown input data.

Multilayer feedforward networks are commonly used to approximate real functions, i.e. for determining weights and parameters of a given neural networks such that a set of given output data matches with a corresponding set of input data, with an approximation error. Some theoretical results have been provided in the related literature (Hetch-Nielsen, 1987) to assure the possibility of approximating any real function satisfying some determined constraints.

Many types of activation function *a* can be used with the above neural network model. In this work, we will use the well-known sigmoid function with the following formula:

$$a(x) = \frac{1}{1 + e^{-\beta x}} \tag{1}$$

where β is a parameter that should be appositely chosen when designing the neural network architecture.

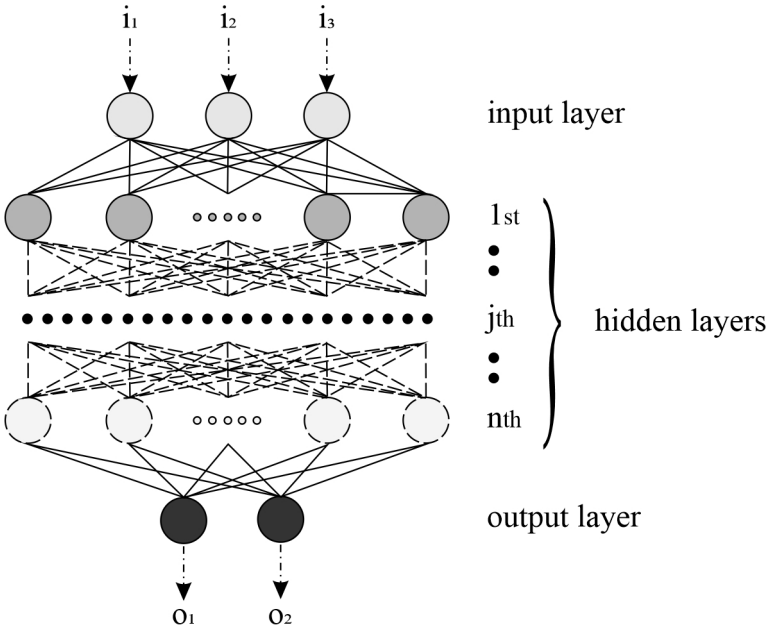

Figure 2 – The architecture of the ANN used to model the hydrological response of plots (Liétor, Castilla La Mancha, Spain).

2.2.2. ANN implementation

In these experiments, we used the Neuroph framework for training the ANN on a data set of real hydrological information. The data set contains 243 tuples of four attributes, namely *i*) treatment, *ii*) precipitation (mm), *iii*) runoff (mm) and *iv*) soil loss (kg/ha). Among the input variables, rainfall intensity has not been deliberately included, although many studies (e.g., Lucas-Borja et al., 2019; Prats et al., 2012), carried out in the same environmental conditions, have demonstrated that, beside the total rainfall, rainfall intensity is the most influential variables explaining runoff generation after fire. This choice is due to the fact that many weather stations (as happen in Spain) are equipped only with rain gauges, which provides daily depths rather than with automated devices, allowing continuous measurements of rainfalls for hourly or sub-hourly intensity calculations. By this way, the ANN seems to have a larger transferability compared to the gauged areas.

The treatment assumes the following discrete values: *Burned+Mulching+No-Logging*, *Burned+No-Mulching+No-Logging*, *Non-Burned*, *Burned+Mulching+Logging* and *Burned+No-Mulching+Logging*.

The attributes *i*) and *ii*) are considered as the neural network inputs, while *iii*) and *iv*) are used as neural network outputs.

2.2.3. Data pre-processing

First, we have processed the data to obtain a suitable dataset to train the neural network. The value of treatment has been transformed into an integer number that takes values between 1 and 5. In particular, *Burned+Mulching+No-logging* = 1, *Burned+No-mulching+No-logging* = 2, *Non-burned* = 3, *Burned+Mulching+Logging* = 4 and *Burned+No-mulching+Logging* = 5. Since some pair of inputs <treatment, precipitation> were associated with different outputs (due to the fact that the same precipitation can produce different runoff volumes, because of many factors, such as the variability of precipitation intensity, soil characteristics in time and space), we averaged in those cases the values of the surface runoff and soil loss. The new dataset is shown in Table 1a.

Then, the data set had to be normalized. Normalization implies that all values from the dataset should take values in the range from 0 to 1. For this purpose, we used the following formula:

$$X_n = \frac{X - X_{min}}{X_{max} - X_{min}} \tag{2}$$

where X is the value that should be normalized, X_n is the normalized value, X_{min} is the minimum value of X and X_{max} is the maximum value of X. Therefore, we obtained the dataset shown in Table 1b.

314 Tables 1a and 1b - The original (a) and normalized (b) datasets used to model the hydrological
315 response of plots through ANNs (Liétor, Castilla La Mancha, Spain).
316
317 (a)

Treatment (input 1)	**Precipitation (mm) (input 2)**	**Runoff volume (mm) (output 1)**	**Soil loss (kg/ha) (output 2)**
1.0	40.0	1.65	68.1
2.0	40.0	2.21	316.3
3.0	40.0	0.00	0.0
1.0	41.0	0.41	145.16
2.0	41.0	0.35	403.09
3.0	41.0	0.00	6.366
1.0	59.0	0.25	158.35
2.0	59.0	0.25	424.01
3.0	59.0	0.03	8.3
4.0	93.8	0.60	5.98
5.0	93.8	0.70	77.73
3.0	93.8	0.08	0.6
4.0	28.0	0.15	8.84
5.0	28.0	0.18	19.52
3.0	28.0	0.02	1.97
4.0	16.8	0.13	9.45
5.0	16.8	0.19	15.91
3.0	16.8	0.00	0.0
4.0	11.6	0.02	7.1

5.0	11.6	0.04	38.48
3.0	11.6	0.01	0.79
4.0	47.4	1.46	48.28
5.0	47.4	1.34	103.25
3.0	47.4	0.03	4.15
4.0	20.7	0.08	22.32
5.0	20.7	0.21	21.72
3.0	20.7	0.03	0.26

318

319

320 (b)

Treatment (input 1)	**Precipitation (input 2)**	**Runoff volume (output 1)**	**Soil loss (output 2)**
0.0	0.345	0.75	0.16
0.25	0.345	1.0	0.74
0.5	0.345	0.0	0.0
0.0	0.358	0.18	0.34
0.25	0.358	0.16	0.95
0.5	0.358	0.0	0.01
0.0	0.577	0.11	0.37
0.25	0.577	0.11	1.0
0.5	0.577	0.013	0.02
0.75	1.0	0.27	0.01
1.0	1.0	0.32	0.18
0.5	1.0	0.04	0.001

0.75	0.199	0.07	0.02
1.0	0.199	0.08	0.05
0.5	0.199	0.009	0.005
0.75	0.063	0.06	0.02
1.0	0.063	0.08	0.04
0.5	0.063	0.0	0.0
0.75	0.0	0.009	0.02
1.0	0.0	0.018	0.09
0.5	0.0	0.004	0.002
0.75	0.435	0.66	0.114
1.0	0.435	0.6	0.24
0.5	0.435	0.013	0.0097
0.75	0.111	0.04	0.53
1.0	0.111	0.095	0.51
0.5	0.111	0.013	$6.0e^{-04}$

321

322

323 Tables 2a and 2b - Runoff volume (a) and soil loss (b) observed and simulated by the ANN used to
324 model the hydrological response of plots through (Liétor, Castilla La Mancha, Spain).

325

326 (a)

Observed runoff (mm)	**Simulated runoff (mm)**	**Error (mm)**
1.65	1.65	0
2.21	2.14	0.07

0	0.025	0.025
0.41	0.39	0.02
0.35	0.35	0
0	0.0084	0.0084
0.25	0.243	0.007
0.25	0.21	0.04
0.03	0.06	0.03
0.6	0.57	0.03
0.7	0.7	0
0.08	0.11	0.03
0.15	0.15	0
0.18	0.21	0.03
0.02	0.0097	0.0103
0.13	0.085	0.045
0.19	0.13	0.06
0	0.007	0.007
0.02	0.072	0.052
0.04	0.11	0.07
0.01	0.0075	0.0025
1.46	1.46	0
1.34	1.33	0.01
0.03	0.00044	0.02956
0.08	0.1	0.02
0.21	0.15	0.06
0.03	0.0075	0.0225

327

328 (b)

Observed soil loss (kg/ha)	Simulated soil loss (kg/ha)	Error (kg/ha)
68.1	85.18	17.08
316.3	320.42	4.12
0	0.38	0.38
145.16	136.49	8.67
403.09	401.96	1.13
6.36	0.42	5.94
158.35	157.69	0.66
424.01	424.01	0
8.3	12.42	4.12
5.98	0.975	5.005
77.73	76.19	1.54
0.6	2.03	1.43
8.84	7.93	0.91
19.52	20.35	0.83
1.97	0.38	1.59
9.45	11.45	2
15.91	24.8	8.89
0	0.72	0.72
7.1	14.96	7.86
38.48	30.4	8.08
0.79	1.02	0.23

48.28	48.76	0.48
103.25	101.93	1.32
4.15	3.985	0.165
22.32	9.54	12.78
21.72	21.88	0.16
0.26	0.55	0.29

329

330

331 *2.2.4. Neural network architecture*

332

333 We adopted the Neuroph, which is an ANN tool, and the *Multi Layer Perceptron* architecture,
334 which is a feedforward ANN (see Section 2). This ANN model maps sets of input data into a set of
335 appropriate output. It consists of multiple layers of nodes in a directed graph, with each layer fully
336 connected to the next one. Except for the input nodes, each node is a neuron with nonlinear
337 activation function.
338 Multilayer Perceptron uses a supervised learning technique called *backpropagation* for the training
339 stage. It is a modification of the standard linear Perceptron, which is not able to distinguish data that
340 not linearly separable, as in our case. We set multi-layer Perceptron 's parameters. The number of
341 input and output neurons was the same as in the training set. Then, we had to choose number of
342 hidden layers, and number of neurons in each layer.
343 The topology of our ANN was chosen as the result of a preliminary study, where several
344 alternatives in terms of number of hidden layers and number of neurons for layer were tested. At the
345 end of this study, the best performance architecture resulted in two hidden layers with 20 neurons in
346 each layer (Figure 3).
347

Figure 3 - The ANN with two hidden layers with 20 following neurons used to model the hydrological response of plots (Liétor, Castilla La Mancha, Spain).

Then we adopted a 'Sigmoid' for transfer function, while, for learning rule, we chose a 'Backpropagation with Momentum'. The momentum is a real value added to speed up the process of learning and to improve the efficiency of the algorithm.

2.2.5. Neural network training

After we have created training set and set the parameters of the neural network, we started to train it.

In our case the maximum error was set to 0.0001, learning rate was set to 0.2 and momentum was set to 0.7. In the first phase, we calculated the total Mean Square Error (MSE). For that purpose, the following formula was used:

$$MSE = \frac{1}{n}\sum_{i=1}^{n}\left(Y_i - \hat{Y}_i\right)^2 \quad (3)$$

where MSE is the arithmetic mean of the squares of the errors $(Y_i - \hat{Y}_i)^2$.

In the following, we will refer to the MSE as the Total Network Error. When this Total Network Error value dropped below the max error, the training was complete. The smaller the error is, the better the obtained approximation is.

372 **2.3. Evaluation of the hydrological prediction capability of ANN**

373

374 The predictions of surface runoff and soil loss provided by the adopted ANN model were compared
375 to the corresponding observations collected in the equipped plots. First, observed and simulated
376 values were visually compared in "scatter-plots". Then, the following indicators, usually adopted in
377 the literature studies dealing with hydrological modelling (e.g., Willmott, 1982; Legates and
378 McCabe, 1999; Loague and Green, 1991; Zema et al., 2017; 2018), were calculated:

379 (i) the main statistics (i.e. the maximum, minimum, mean and standard deviation of both the
380 observed and simulated values);

381 (ii) the coefficients of determination (r^2), efficiency (E, Nash and Sutcliffe, 1970) and residual
382 mass (CRM, also knowns as "percent bias", PBIAS); and

383 (iii) the Root Mean Square Error (RMSE).

384 The related equations for the calculation of these indicators are reported by Zema et al. (2012),
385 Krause et al. (2005), Moriasi et al. (2007) and Van Liew and Garbrecht (2003).

386 To summarise, the model performance can be evaluated as follows:

387 - the closer the statistics, the more accurate the model predictions;

388 - values of r^2, ranging from 0 to 1, over 0.5 indicate reasonable model performance (Santhi et al.,
389 2001; Van Liew et al., 2003; Vieira et al., 2018);

390 - E, in the range $-\infty$ to 1, is negative for a model giving poor predictions, ≥ 0.35 for a satisfactory
391 model and ≥ 0.75 for a good performance (Zema et al., 2017);

392 - RMSE, which should be as closest as possible to zero (no errors between predictions and
393 observations), less than half the standard deviation of the measured data are considered good
394 (Singh et al., 2004);

395 - CRM/PBIAS, which, if positive, indicates model underestimation, whereas, if negative, model
396 overestimation (Gupta et al., 1999), must be below 0.25 or 0.55 for good runoff and soil loss
397 predictions, respectively, according to Moriasi et al. (2007).

3. RESULTS AND DISCUSSIONS

3.1. Runoff and soil erosion observations

During the observation period, nine events were monitored, for which precipitation depth and mean intensity were in the range 11.6-93.8 mm and 0.98-28.0 mm/h. The monitored events were only those producing surface runoff and erosion. As expected, all burned plots gave runoff volumes and soil loss significantly (at $p < 0.05$) much higher than non-burned soils (control), for which the mean runoff and soil loss were 0.02 ± 0.03 mm and 2.49 ± 3.07 kg/ha (mean ± standard deviation). Also Gimeno-García et al. (2007), studying the soil's hydrological response after wildfires in Mediterranean shrublands, showed that total runoff and sediment yield in the first post-fire year (19.43 mm and 0.56 kg/m^2 in the intense fire) contrast with the very low runoff (3.82 mm) and soil loss (0.08 kg/m^2) in control plots. In a different Mediterranean landscape, Mayor et al (2007) found that total runoff and sediment yield in the burned catchment (35 mm and 4.56 kg/ha, respectively) were considerably greater than in the unburned catchment (0.03 mm, and 0.12 kg/ha). Key casual factors enhancing runoff and soil loss are the reduction in infiltration and some combination of sealing, soil water repellency, loss of surface cover, and disaggregation due to loss of soil organic matter (Neary et al., 2005).

Mulching reduced the hydrological response of the B+M+NL soils (mean runoff of 0.26 ± 0.54 mm as well as soil loss of 41.3 ± 66.6 kg/ha soils) compared to B+NM+NL plots (mean runoff of 0.31 ± 0.72 mm and soil loss of 127 ± 193 kg/ha) (Figure 4a and 4b). The differences were significant for soil erosion, but not for runoff. The efficacy of mulch application to control soil erosion is in accordance with Bautista et al. (2009), who highlighted the immediate increase of ground cover in mulch application, which result in an effective soil protection for the first rain events after fire.

424 The effects of logging on burned soils (mulched or not) anywhere not appreciably different between
425 the plots, since the differences in surface runoff and soil loss were not significant (at $p < 0.05$).
426 More specifically, B+NM+L plots gave higher runoff (on the average 0.30 ± 0.45 mm) and soil loss
427 (on the average 30.7 ± 36.7 kg/ha) compared to B+M+L soils (mean runoff of 0.27 ± 0.48 mm and
428 soil loss of 11.3 ± 15.5 kg/ha) (Figure 4a and 4b). This is in accordance with other authors that did
429 not report a significantly negative effect of logging in soil parameters (Fernández and Vega, 2016).
430 The type of machinery used during forest operations could also explain this. As Lucas-Borja et al.
431 (2018) demonstrated, the use of not heavy machinery with air tires generates not negative impact on
432 soil and reduce soil compaction in comparison to chain tires.
433 It is worth to highlight that a temporal gradient in runoff generation mechanism was found for the
434 B+NM+NL and B+M+NL (regardless of the treatment), indicating a decrease of the hydrological
435 response of all soils throughout the time elapsed from fire. In other words, the largest runoff - and
436 thus soil loss - was produced by the rainfall events occurring immediately after the wildfire, as
437 shown by the decrease of the runoff coefficients (data not shown). This has been observed in the
438 first and second storms in the season immediately after wildfires by several authors (e.g., de Dios
439 Benavides-Solorio and MacDonald, 2005; DeBano et al., 1998; MacDonald et al., 2000; Robichaud
440 and Brown, 1999). The large increase in the runoff coefficients just after fire has been attributed to
441 changes in soil hydrological properties, such as the development of a water-repellent layer at or near
442 the soil surface, which prevents infiltration and induces overland flow (DeBano et al., 1970;
443 Shakesby et al., 2000). In addition, this fact might be explained by the vegetation (mainly shrubs
444 and herb) recovery after fires that performed better than litter in order to stop runoff generation. The
445 complex system of vegetation patches in control plots which is highly disconnected that influence
446 of semi-arid Mediterranean vegetation on runoff generation has been widely reported in previous
447 studies (i.e. Dunjó et al., 2004).
448

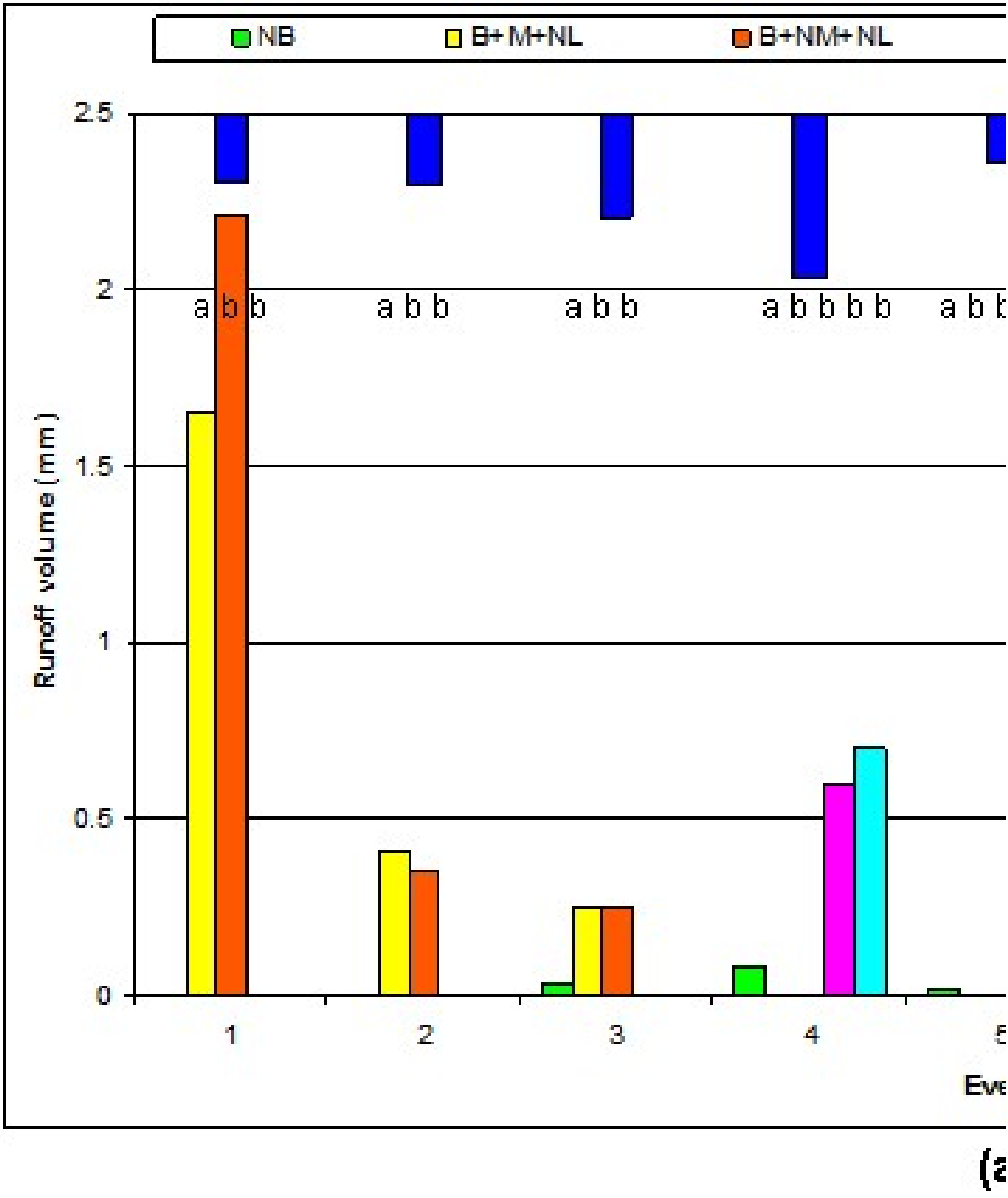

449

450 Figures 4a and 4b - Precipitation, runoff volumes (a) and soil losses (b) observed in the
451 experimental plots (Liétor, Castilla La Mancha, Spain) (NB = Non-Burned; B+M+NL =
452 Burned+Mulching+No-Logging; B+NM+NL = Burned+No-Mulching+No-Logging; B+M+L =

453 Burned+Mulching+Logging; B+NM+L = Burned+No-Mulching+Logging; different lower case
454 letters indicate statistically significant differences at $p < 0.05$).
455
456 **3.2. Hydrological modelling by ANN**
457
458 First, we train the neural network for the first output. After 250000 iterations we obtained a Total
459 Mean Square Error drop down to a specified level of 0.0001, which means that training process was
460 successful.
461
462 *3.2.1. Neural Network Approximation*
463
464 A Total Mean Square Error of 1.965 e^{-4} in simulating the runoff volume was achieved (Figure 5a),
465 which certainly is a very good result, because our goal is to get the total error to be as small as
466 possible. In more detail, Table 2a reports the observed (desired output) and simulated (ANN output)
467 runoff values and the related differences the trained neural network produced. Looking at the
468 individual errors, we can observe that most of them are at the low level, below 0.1. MAE was equal
469 to 0.025 mm. So we can conclude that this type of neural network architecture is the best choice.
470 We used the same neural network shown in Figure 2. Also in this case, we set the maximum error to
471 0.0001, the learning rate to 0.2 and the momentum to 0.7. After 175000 iterations we obtained a
472 total MSE drop down to a specified level of 0.0001, which means that training process was
473 successful and that now we can exploit this trained neural network (Figure 5b). The Total Mean
474 Square Error for this second neural network was 1.78 e^{-4}. The relative error on the individual soil
475 loss between the observations and the simulations (Table 2b) was lower than 17.1 kg/ha while MAE
476 was equal to 3.57 kg/ha.
477

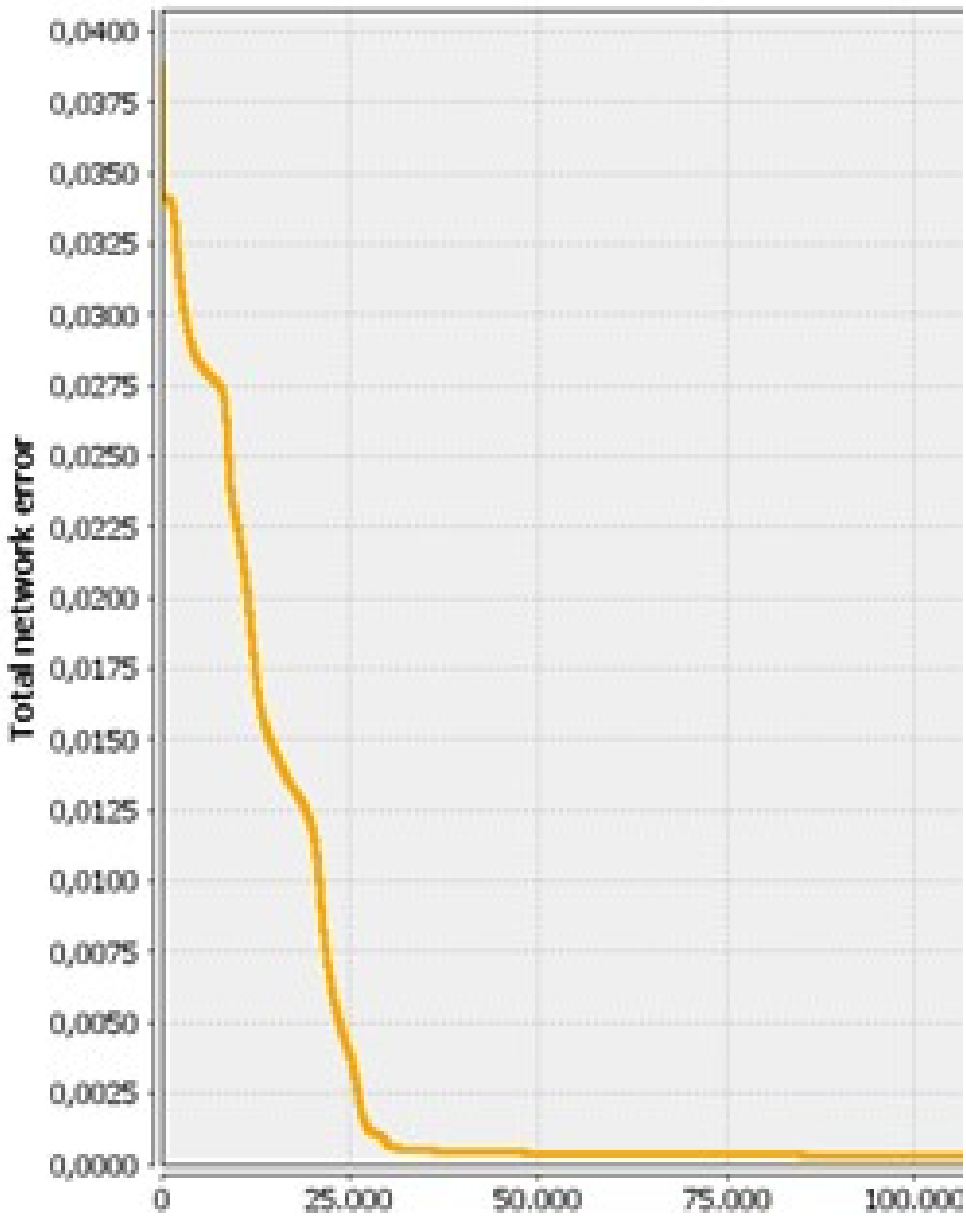

478

479 Figures 5a and 5b - Total Network Error (equal to the Total MSE, Mean Square Error for runoff
480 volume (a) and soil loss (b) simulated by the ANN used to model the hydrological response of plots
481 (Liétor, Castilla La Mancha, Spain).

482

483 *3.2.2. Evaluation of the ANN prediction capability*

484

485 The scatter plots of Figure 6a and 6b show a very close agreement between the predictions provided
486 by ANN and the corresponding observations collected at the plots for both surface runoff volumes
487 and soil loss for all the experimental conditions (control, burned and treated/not treated soils).

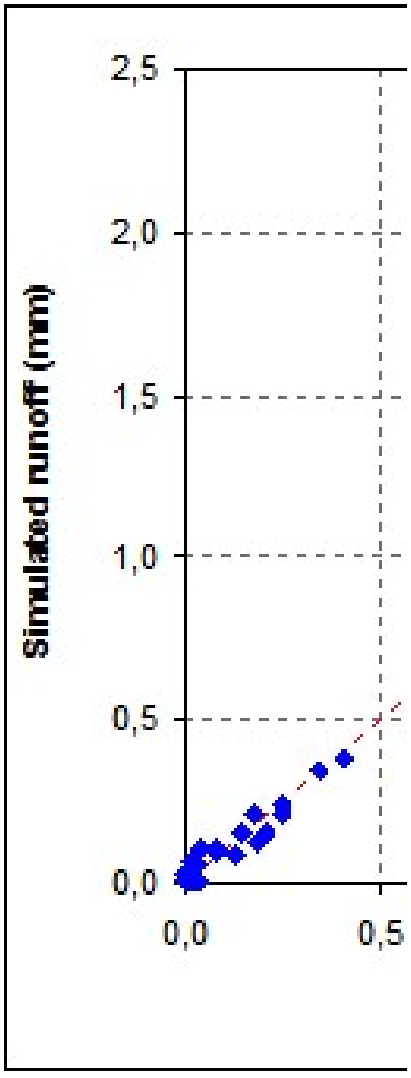

488

489

490 Figures 6a and 6b - Scatter plot of the observed vs simulated (by ANN) runoff volumes (a) and soil
491 loss (b) in the experimental plots (Liétor, Castilla La Mancha, Spain).

This qualitative agreement is confirmed by the values of the indicators adopted for the quantitative assessment of ANN prediction capability. In general, when the ANN performance is evaluated by aggregating all the soil conditions, the statistics (i.e., mean, standard deviation, minimum and maximum) were practically equal for both runoff and soil loss. Only very small differences were found for the maximum runoff (under 3.2%) and the minimum soil loss (modelled as zero against a mean value of 0.38 kg/ha). Moreover, the model efficiency and RMSE are good and the coefficient of determination equal to one, while the CRM (equal to 0.01) indicates a very small model underestimation of the observations (Table 3).

A more detailed analysis of the ANN performance, carried out separately for the individual soil conditions (burned/unburned) and treatments (mulching/logging) highlighted that (Table 3):

- the observed and predicted mean values of both runoff and soil loss are practically the same and the maximum difference (16.2%, however under the acceptance threshold) is detected for soil loss prediction in B+M+L plots;
- the lower agreement between observations and predictions was found in the maximum runoff (with differences lower than 32%) and in the minimum soil loss (below 112%); for the latter, in same cases the ANN predicted soil losses equal to zero also in the case of observed erosion; instead, for the maximum soil losses, only in one case (for the B+M+L plots) the difference with the corresponding observation was more than 20%.

511 Table 3 - Values of the criteria adopted for ANN evaluation in the experimental plots (Liétor, Castilla La Mancha, Spain).

512

Treatment	Number of events	Value	Mean	Minimum	Maximum	Standard Deviation	E	CRM	r^2	RMSE
			(mm or kg/ha)				(-)	(-)	(-)	(mm or kg/ha)
RUNOFF VOLUME										
ALL DATA	27	Observed	0.39	0.00	2.21	0.59	-	-	-	-
		Simulated	0.38	0.00	2.14	0.58	1.00	0.01	1.00	0.03
NB	9	Observed	0.57	0.00	2.21	0.80	-	-	-	-
		Simulated	0.56	0.01	2.14	0.78	1.00	0.01	1.00	0.03
B+M+NL	3	Observed	0.46	0.08	0.70	0.33	-	-	-	-
		Simulated	0.46	0.11	0.70	0.31	0.99	0.00	1.00	0.02
B+NM+NL	3	Observed	0.12	0.02	0.18	0.09	-	-	-	-
		Simulated	0.12	0.01	0.21	0.10	0.93	-0.06	0.99	0.02
B+M+L	6	Observed	0.07	0.00	0.19	0.08	-	-	-	-
		Simulated	0.07	0.01	0.13	0.05	0.55	-0.06	0.56	0.05
B+NM+L	6	Observed	0.53	0.03	1.46	0.68	-	-	-	-

		Simulated	0.51	0.00	1.46	0.69	1.00	0.03	1.00	0.03
SOIL LOSS										
ALL DATA	27	Observed	70.96	0.00	424.01	120.84	-	-	-	-
		Simulated	70.99	0.38	424.01	120.96	1.00	0.00	1.00	5.60
NB	9	Observed	169.96	0.00	424.01	170.74	-	-	-	-
		Simulated	171.00	0.38	424.01	170.21	1.00	-0.01	1.00	6.98
B+M+NL	3	Observed	196.89	8.30	424.01	210.52	-	-	-	-
		Simulated	198.04	12.42	424.01	208.74	1.00	-0.01	1.00	2.41
B+NM+NL	3	Observed	10.11	1.97	19.52	8.84	-	-	-	-
		Simulated	9.55	0.38	20.35	10.08	0.97	0.06	1.00	1.16
B+M+L	6	Observed	11.96	0.00	38.48	14.26	-	-	-	-
		Simulated	13.89	0.72	30.40	12.15	0.79	-0.16	0.82	5.93
B+NM+L	6	Observed	33.33	0.26	103.25	38.25	-	-	-	-
		Simulated	31.11	0.55	101.93	38.85	0.98	0.07	0.98	5.25

Notes: NB = Non-Burned; B+M+NL = Burned+Mulching+No-Logging; B+NM+NL = Burned+No-Mulching+No-Logging; B+M+L = Burned+Mulching+Logging; B+NM+L = Burned+No-Mulching+Logging.

515 As regards the other model performance indicators, the following considerations can be drawn
516 (Table 3):
517 - ANN showed a very slight tendency to overestimate or underestimate the hydrological
518 observations (for instance, overestimation of runoff in B+NM+L and B+NM+L plots, CRM = -0.06
519 as well as underestimation of soil loss in B+NM+NL and B+NM+L, CMR = 0.06-0.07), as shown
520 by the very small negative or positive values of CMR;
521 - for all the soil conditions/treatments and both for runoff and soil loss predictions, E, r^2 and RMSE
522 attained good values (that is, very close to one for E and r^2, and to zero for RMSE), except for the
523 B+M+L plots;
524 - for the latter soil condition and treatment, the worst performance of the ANN was found for both
525 runoff and erosion predictions (see values of E, r^2 and RMSE). Presumably, in soil subjected to
526 logging, the impacts of machinery wheels on soil determine the formation of small rills, in which
527 small volumes of water and sediments are stored and do not feed runoff. Since, in general, many
528 models find difficulties in modelling rill erosions (e.g., Aksoy and Kavvas, 2005), this behaviour
529 could be common with ANN.
530 However, on account of E, r^2 and RMSE values, the prediction capability of the ANN can be
531 considered as satisfactory to good for runoff and good for soil loss. This indicates that a soil
532 disturbance due to more than two factors (in our case wildfire, mulching and logging) founds some
533 difficulties in being simulated by ANN, which however does not compromise the generally good
534 model performances.
535 The runoff and erosion prediction capacity provided by ANNs appears to be very satisfactory in the
536 experimental conditions and this is even more appreciable if we make comparisons with other
537 conceptual models. For instance, limiting the evaluation criteria to model efficiency, the very high
538 E coefficients of this study (close to 0.99) is noticeably higher compared to the maximum values (E
539 from -10 to 0.93) reported in the studies of Vieira et al. (2014), Fernandez et al. (2010) and Hosseini
540 et al. (2018), who applied the MMF model for predicting runoff and erosion at seasonal and annual

541 scales on soils of Iberian Peninsula, burned by fires of different severity and subjected to different
542 post-fire treatments. Fernandez et al. (2010) and Fernandez and Vega (2016) found some
543 inaccuracies of the RUSLE model (shown by a negative E) for predicting annual soil erosion from
544 burned soils of NW Spain, since the K factor did not allow to reflect the changes on soil
545 permeability and structure after fire, while the annual soil loss predictions achieved by Vieira et al.
546 (2018) applying RUSLE in north-central Portugal were more satisfactory (E = 0.63-0.70).
547 Contrasting results in annual erosion prediction capacity provided by PESERA model applied in
548 burned plots were shown by coefficients E of 0.33 (Fernandez and Vega, 2016) or 0.73-0.85 (Vieira
549 et al., 2018).
550 The ANN models focus on mathematical solutions over process representation, such as the
551 empirical models do. In other words, it is a "black box" approach, which estimates runoff and soil
552 loss, but does not gives information about the physical factors underlying the hydrological
553 processes. Nonetheless, empirical models are frequently used in preference to more complex
554 models as they can be implemented in situations with limited data and parameter inputs, and are
555 particularly useful as a first step in identifying sources of water, sediments and pollutants (Merritt et
556 al., 2003). However, the main goal of technicians and land planners is first the knowledge of the
557 runoff and erosion rates and then the selection of the most suitable treatment to reduce the
558 unsustainable rates, rather than a detailed comprehension of the hydrological processes. For
559 stakeholders or government agencies, who may be responsible for land and water management on a
560 national or regional basis, the complex models are prohibitive in terms of the time required to
561 develop and implement them (Fu et al., 2018). Since the data requirements of any model increase
562 with the model complexity, models that are less complex than the physically-based models, such as
563 the empirical models (Aksoy and Kavvas, 2005), are more indicated for use in burned areas of
564 Mediterranean forests, which are often data-poor environments. Low-data demanding models are
565 based primarily on the analysis of observations and seek to characterise response from these data
566 (Wheater et al., 1993). The simplest models are regression equations between climatic variables

(such as precipitation volumes and intensities) and runoff/erosion rates. However, in the experimental areas, linear regressions were not able to predict with accuracy runoff volumes and soil loss from simple observations of precipitation. As a matter of fact, very low coefficients of determination were found by regressing both runoff volumes and soil loss to precipitation depth and intensity in non-burned soils as well as in burned plots (mulched or not) (Figure 7). This presumably happened, since these simple models ignore the inherent non-linearities in the hydrological processes and employ unrealistic assumptions about the physics (Wheater et al., 1993). Conversely, the ANNs, which require only precipitation as input, but use a more complex mathematical structure, were successful in capturing the output hydrological variables from the observational input data, as shown by the very good prediction capacity detected for the ANNs in the experimental conditions of this study.

Therefore, the main advantages of the ANN use are in such environmental contexts are the low input requirement in comparison to the more complex physically-based models and, at the same time, the prediction accuracy in comparison to the simpler empirical models. This is appreciated by land planners and forest managers, who have a powerful prediction tool easy to be used in data-poor environment, as often the Mediterranean forests are.

However, further experimental tests are needed to assure ANN applicability to these climatic, geomorphological and ecological contexts and to upscale the model applications from the plot to the watershed scale; for instance, a larger database of rainfall/runoff events may make the ANN prediction capacity more accurate. On the other hand, a larger and general use of ANN for hydrological predictions requires more experimental investigations in other environmental contexts (different for climate and geomorphology), which should assure a large transferability of this modelling tool for hydrological and ecological management in forest ecosystems potentially prone to fire. If simulations of runoff and erosion remain good also out of the experimental conditions of this study after fire, the availability of powerful ANNs can support landscape planners not only in control the fire risk in forestland, but also in identifying the most efficient countermeasures to limit

593 ecosystem degradation. Conversely, in the case of less accurate hydrological predictions, other
594 important variables - of easy measurement or estimation, - influencing the runoff and erosion
595 generation mechanisms should be implemented when an ANN is designed, such as the rainfall
596 intensity, vegetal cover and texture of soils. Therefore, estimations of water flows and soil erosion
597 using ANN decrease the costs and the studies time otherwise required by hydrological models of
598 other nature.
599

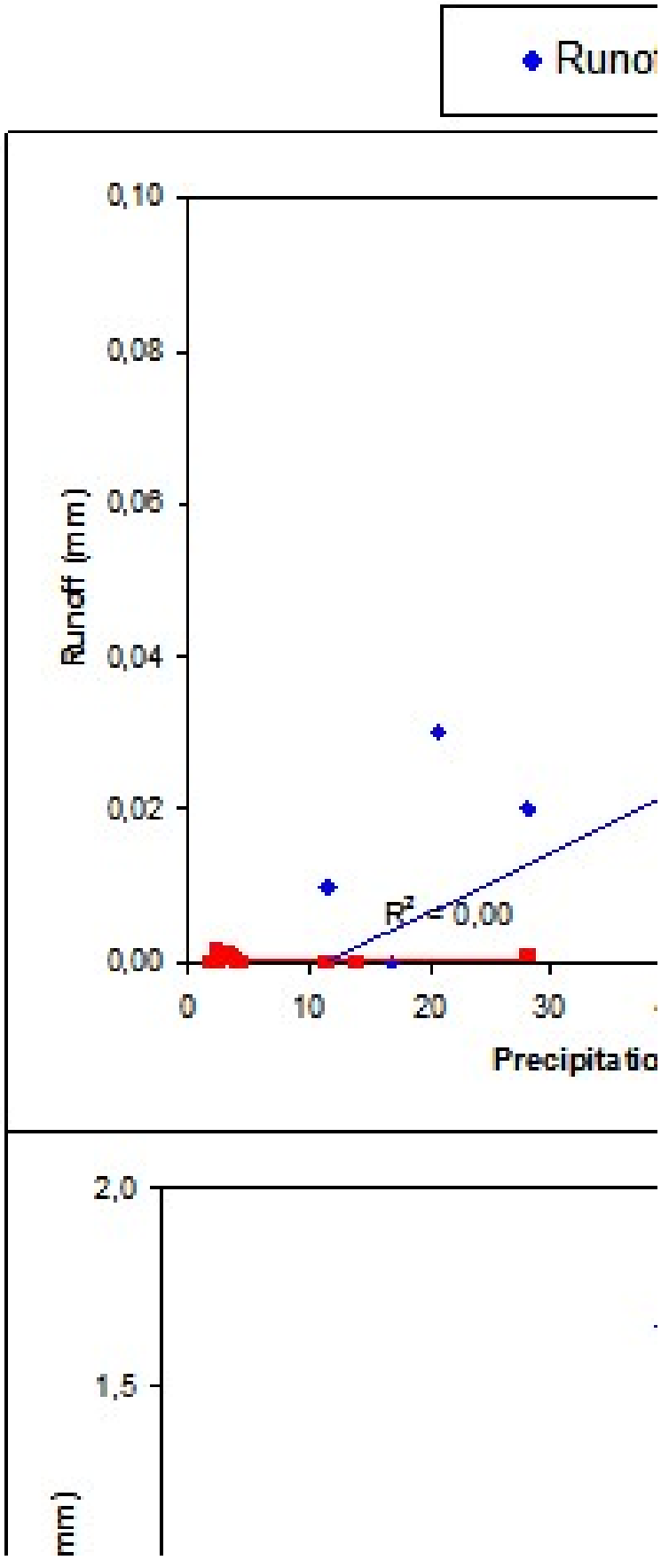
Runo
0,10
0,08
0,06
0,04
0,02
0,00
Runoff (mm)
R² = 0,00
0
10
20
30
Precipitatio
2,0
1,5
mm)

600

Figure 7 - Linear regression between runoff volumes and precipitation depth as well as soil loss and maximum 1-h precipitation intensity in the experimental non-burned (a), burned and mulched (b) and burned and non-mulched (c) plots (Liétor, Castilla La Mancha, Spain).

4. CONCLUSIONS

The evaluation of the ANN for hydrological modelling in the forest plots subject to wildfire showed that the runoff and erosion prediction capability is in general very good. The ANN performance was exceptionally high for all the experimental conditions, since the model efficiency and the coefficient of determination was equal to one, while the very low CRM indicated a negligible underestimation of the observations. The ANN proposed is also very robust, in the sense that its performance is exceptionally high for all the experimental conditions (burned or non-burned soils) and treatments (mulching and/or logging or not), with only one exception (that is, in the condition where the soil disturbance is higher).

Overall, this modelling approach only needs precipitation data (whose measuring equipment are available also in forestlands) as well as a reasonable set of rainfall-runoff observations to train the ANN. Therefore, the use of ANNs for hydrological predictions in burned areas of Mediterranean forests seems to be a useful decision support system for the integrated assessment and management of forested watersheds.

REFERENCES

Aksoy, H. and Kavvas, M.L., 2005. A review of hillslope and watershed scale erosion and sediment transport models. Catena 64(2-3), 247-271.

627 Albaradeyia, I., Hani, A., Shahrour, I., 2011. WEPP and ANN models for simulating soil loss and
628 runoff in a semi-arid Mediterranean region. Environmental monitoring and assessment 180(1-4),
629 537-556.
630 Allué, J.L., 1990. Atlas fitoclimático de España. Taxonomías. Ministerio de Agricultura, Pesca y
631 Alimentación. INIA Madrid, Spain.
632 Asadi, H., Shahedi, K., Jarihani, B., Sidle, R.C., 2019. Rainfall-runoff modelling using hydrological
633 connectivity index and artificial neural network approach. Water 11(2), 212.
634 ASCE Task Committee, 2000. Artificial neural networks in hydrology. I. Preliminary concepts. J
635 Hydraul Eng ASCE 5(2), 115–123.
636 Bautista, S., Robichaud, P.R., Bladé, C., 2009. Post-fire mulching. Fire Eff. Soils Restor. Strateg.
637 Sci. Publ. Enfield, NH. 353–372.
638 Benavides-Solorio, J.D. and Macdonald, L.H., 2005. Measurement and prediction of post-fire
639 erosion at the hillslope scale, Colorado Front Range. International Journal of Wildland Fire 14, 457-
640 474.
641 Certini, G., 2014. Fire as a soil-forming factor. Ambio 43, 191–195.
642 Dawson, C.W. and Wilby, R., 1998. An artificial neural network approach to rainfall-runoff
643 modelling. Hydrological Sciences Journal 43(1), 47-66.
644 Esteves, T.C.J., Kirkby, M.J., Shakesby, R.A., Ferreira, A.J.D., Soares, J.A.A., Irvine, B.J.,
645 Fernández, C., Vega, J.A., Vieira, D.C.S., 2010. Assessing soil erosion after fire and rehabilitation
646 treatments in NW Spain: performance of RUSLE and revised Morgan–Morgan–Finney
647 models. Land degradation & development 21(1), 58-67.
648 Fernández, C. and Vega, J.A., 2016. Evaluation of RUSLE and PESERA models for predicting soil
649 erosion losses in the first year after wildfire in NW Spain. Geoderma 273, 64–72..
650 Ferreira, C.S.S., Coelho, C.O.A., Bento, C.P.M., Carreiras, M.A., 2012. Mitigating land degradation
651 caused by wildfire: application of the PESERA model to fire affected sites in central Portugal.
652 Geoderma 191, 40-50.

653 Fu, B., Merritt, W.S., Croke, B.F., Weber, T., Jakeman, A.J., 2018. A review of catchment-scale
654 water quality and erosion models and a synthesis of future prospects. Environmental modelling &
655 software 114, 85-97.
656 Gholami, V., Booij, M.J., Tehrani, E.N., Hadian, M.A., 2018. Spatial soil erosion estimation using
657 an artificial neural network (ANN) and field plot data. Catena 163, 210-218.
658 Gimeno-García E., Andreu V., Rubio J.L., 2007. Influence of vegetation recovery on water erosion
659 at short and medium-term after experimental fires in a Mediterranean shrubland. Catena 69, 150-
660 160.
661 Haykin S. , 1994. Neural Networks: A Comprehensive Foundation. Prentice Hall, USA.
662 Hetch-Nielsen, R., 1987. Kolmogorov's mapping neural network existence theorem. In Proceedings
663 of the International Conference on Neural Networks, vol. 3, 11-14, New York, USA.
664 Hosseini, M., Nunes, J. P., Pelayo, O. G., Keizer, J.J., Ritsema, C., Geissen, V., 2018. Developing
665 generalized parameters for post-fire erosion risk assessment using the revised Morgan-Morgan-
666 Finney model: A test for north-central Portuguese pine stands. Catena 165, 358-368.
667 Hsu, K.-L., Gupta, H.V., Sorooshian, S., 1995. Artificial neural network modeling in rainfall–runoff
668 process. Water Resources Research 31(10), 2517–2530.
669 Kim, M. and Gilley, J.E., 2008. Artificial Neural Network estimation of soil erosion and nutrient
670 concentrations in runoff from land application areas. Computers and electronics in
671 agriculture 64(2), 268-275.
672 Kottek, M., Grieser, J., Beck, C., Rudolf, B., Rubel, F., 2006. World Map of the Köppen-Geiger
673 climate classification updated. Meteorol. Z. 15, 259-263.
674 Larsen, I.J., MacDonald, L.H., Brown, E., Rough, D., Welsh, M.J., Pietraszek, J.H., Schaffrath, K.,
675 2009. Causes of post-fire runoff and erosion: water repellency, cover, or soil sealing? Soil Science
676 Society of America Journal 73(4), 1393-1407.
677 Legates, D.R. and McCabe, G.J., 1999. Evaluating the use of “goodness of fit” measures in
678 hydrologic and hydroclimatic model validation. Water Resources Research 35, 233-241.

679 Licznar, P. and Nearing, M.A., 2003. Artificial neural networks of soil erosion and runoff
680 prediction at the plot scale. Catena 51(2), 89-114.
681 Loague, K. and Green, R.E., 1991. Statistical and graphical methods for evaluating solute transport
682 models: Overview and application. Journal of Contaminant Hydrology 7, 51-73.
683 Lucas-Borja, M.E., Plaza-Álvarez, P.A., Gonzalez-Romero, J., Sagra, J., Alfaro-Sánchez, R., Zema,
684 D.A., de Las Heras, J., 2019. Short-term effects of prescribed burning in Mediterranean pine
685 plantations on surface runoff, soil erosion and water quality of runoff. Science of The Total
686 Environment 674, 615-622.
687 Lucas-Borja, M.E., González-Romero, J., Plaza-Álvarez, P.A, Sagra, J., Gómez M.E., Moya, D.,
688 Cerdà, A., de las Heras, J., 2018. The impact of straw mulching and salvage logging on post-fire
689 runoff and soil erosion generation under Mediterranean climate conditions. Science of the Total
690 Environment 654, 441-451.
691 Lucas-Borja, M.E., Zema, D.A., Carrà, B.G., Cerdà, A., Plaza-Alvarez, P.A., Cózar, J.S., de las
692 Heras, J., 2018. Short-term changes in infiltration between straw mulched and non-mulched soils
693 after wildfire in Mediterranean forest ecosystems. Ecological Engineering 122, 27-31.
694 Mayor, A.G., Bautista, S., Llovet, J., Bellot, J., 2007. Post-fire hydrological and erosional responses
695 of a Mediterranean landscape: Seven years of catchment-scale dynamics. Catena 71, 68–75.
696 Merritt, W.S., Letcher, R.A., Jakeman, A.J., 2003. A Review of Erosion and Sediment Transport
697 Model. Environmental Modelling and Software 18, 761-799
698 Moody, J.A., Shakesby, R.A., Robichaud, P.R., Cannon, S. H., Martin, D.A., 2013. Current
699 research issues related to post-wildfire runoff and erosion processes. Earth-Science Reviews 122,
700 10-37.
701 Morales, H.A., Navar, J., Dominguez, P.A., 2000. The effect of prescribed burning on surface
702 runoff in a pine forest stand of Chihuahua, Mexico. Forest Ecol Manag 137, 199–207

703 Moriasi, D.N., Arnold, J.G., Van Liew, M.W., Bingner, R.L., Harmel, R.D., Veith, T.L., 2007.
704 Model evaluation guidelines for systematic quantification of accuracy in watershed
705 simulations. Transactions of the ASABE 50 (3), 885-900.
706 Nash, J.E. and Sutcliffe, J.V., 1970. River flow forecasting through conceptual models: Part I. A
707 discussion of principles. Journal of Hydrology 10, 282-290.
708 Neary, D.G., Ryan, K.C., DeBano, L.F., 2005. Wildland fire in ecosystems: effects of fire on soils
709 and water. Gen. Tech. Rep. RMRS-GTR-42-vol. 4. Ogden, UT US Dep. Agric. For. Serv. Rocky
710 Mt. Res. Station. 250 p. 42.
711 Plaza-Álvarez, P.A., Lucas-Borja, M.E., Sagra, J., Zema, D.A., González-Romero, J., Moya, D., De
712 las Heras, J., 2019. Changes in soil hydraulic conductivity after prescribed fires in Mediterranean
713 pine forests. Journal of Environmental Management 232, 1021-1027.
714 Prats, S.A., MacDonald, L.H., Monteiro, M., Ferreira, A.J., Coelho, C.O., Keizer, J.J., 2012.
715 Effectiveness of forest residue mulching in reducing post-fire runoff and erosion in a pine and a
716 eucalypt plantation in north-central Portugal. Geoderma 191, 115-124.
717 Prats, S.A., MacDonald, L.H., Monteiro, M., Ferreira, A.J.D., Coelho, C.O.A., Keizer, J.J., 2012.
718 Effectiveness of forest residue mulching in reducing post-fire runoff and erosion in a pine and a
719 eucalypt plantation in north-central Portugal. Geoderma 191, 115–124.
720 Riad, S., Mania, J., Bouchaou, L., Najjar, Y., 2004. Rainfall-runoff model usingan artificial neural
721 network approach. Mathematical and Computer Modelling 40(7-8), 839-846.
722 Robichaud, P.R., Elliot, W.J., Pierson, F.B., Hall, D.E., Moffet, C.A., Ashmunm L.E., 2007.
723 Erosion risk management tool (ERMiT) user manual, version 2006.01.18. US Department of
724 Agriculture, Forest Service, Rocky Mountain Research Station, General Technical Report RMRS-
725 GTR- 188., Fort Collins, Colorado. USA.
726 Robichaud, P.R., 2000. Fire effects on infiltration rates after prescribed fire in Northern Rocky
727 Mountain forests, USA. Journal of Hydrology 231, 220-229.

728 Santhi, C., Arnold, J.G., Williams, J.R., Dugas, W.A., Srinivasan, R., Hauck, L.M., 2001.
729 Validation of the SWAT model on a large river basin with point and nonpoint sources. J. Am.
730 Water Resour. Assoc. 37 (5), 1169–1188.
731 Shakesby, R.A., 2011,. Post-wildfire soil erosion in the Mediterranean: review and future research
732 directions. Earth-science reviews, 105(3-4), 71-100.
733 Sharma, S.K. and Tiwari, K.N., 2009. Bootstrap based artificial neural network (BANN) analysis
734 for hierarchical prediction of monthly runoff in Upper Damodar Valley Catchment. Journal of
735 hydrology 374(3-4), 209-222.
736 Singh, J., Knapp, H.V., Demissie, M., 2004. Hydrologic modeling of the Iroquois River watershed
737 using HSPF and SWAT. ISWS CR 2004-08. Champaign, Ill.: Illinois State Water Survey.
738 http://www.sws.uiuc.edu/pubdoc/CR/ISWSCR2004-08.pdf (Accessed 14 February 2018).
739 Sudheer, K.P., Gosain, A.K., Ramasastri, K.S., 2002. A data-driven algorithm for constructing
740 artificial neural network rainfall-runoff models. Hydrological processes 16(6), 1325-1330.
741 Tokar, A.S. and Johnson, P.A., 1999. Rainfall runoff modeling using artificial neural networks.
742 Journal of Hydrologic Engineering 4 (3), 232–239.
743 Van Liew, M.W., Arnold, J.G., Garbrecht, J.D., 2003. Hydrologic simulation on agricultural
744 watersheds: choosing between two models. Trans. ASAE 46 (6), 1539–1551.
745 Van Liew, M.W and Garbrecht, J., 2003. Hydrologic simulation of the Little Washita River
746 experimental watershed using SWAT. Journal of the American Water Resources Association
747 Vega, J.A., Fernández, C., Fontúrbel, M.T., González-Prieto, S.J., Jiménez, E., 2014. Testing the
748 effects of straw mulching and herb seeding on soil erosion after fire in a gorse shrubland. Geoderma
749 223–225, 79–87.
750 Vega, J.A., Fontúrbel, M.T., Merino, A., Fernández, C., Ferreiro, A., Jiménez, E., 2013. Testing the
751 ability of visual indicators of soil burn severity to reflect changes in soil chemical and microbial
752 properties in pine forests and shrubland. Plant and Soil 369, 73–91.

753 Vieira, D.C.S., Prats, S.A., Nunes, J.P., Shakesby, R.A., Coelho, C.O.A., Keizer, J.J., 2014.
754 Modelling runoff and erosion, and their mitigation, in burned Portuguese forest using the revised
755 Morgan-Morgan-Finney model. For. Ecol. Manag. 314, 150–165.
756 Vieira, D.C.S., Serpa, D., Nunes, J.P.C., Prats, S.A., Neves, R., Keizer, J.J., 2018. Predicting the
757 effectiveness of different mulching techniques in reducing post-fire runoff and erosion at plot scale
758 with the RUSLE, MMF and PESERA models. Environmental Research 165, 365-378.
759 Wheater, H.S., Jakeman, A.J., Beven, K.J., 1993. Progress and directions in rainfall-runoff
760 modelling. In: Jakeman, A.J., Beck, M.B., McAleer, M.J. (Eds.), Modelling Change in
761 Environmental Systems. John Wiley and Sons, Chichester, USA, 101-132.
762 Willmott, C.J., 1982. Some comments on the evaluation of model performance. Bulletin of
763 American Meteorological Society 63(11), 1309-1313.
764 Wischmeier, W.H. and Smith, D.D. (1978) Predicting Rainfall Erosion Losses: A Guide to
765 Conservation Planning. Science, US Department of Agriculture Handbook, No. 537, Washington
766 DC, USA.
767 Yusof, M.F., Azamathulla, H.M., Abdullah, R., 2014. Prediction of soil erodibility factor for
768 Peninsular Malaysia soil series using ANN. Neural Computing and Applications 24(2), 383-389.
769 Zema, D.A., Bingner, R.L., Govers, G., Licciardello, F., Denisi, P., Zimbone, S.M., 2012.
770 Evaluation of runoff, peak flow and sediment yield for events simulated by the AnnAGNPS model
771 in a Belgian agricultural watershed. Land Degradation and Development 23(3): 205-215.
772 Zema, D.A., Labate, A., Martino, D., Zimbone, S.M., 2017. Comparing Different Infiltration
773 Methods of the HEC-HMS Model: The Case Study of the Mésima Torrent (Southern Italy). Land
774 Degradation & Development 28(1), 294-308.
775 Zema, D.A., Lucas-Borja, M.E., Carrà, B.G., Denisi, P., Rodrigues, V.A., Ranzini, M., Zimbone, S.
776 M., 2018. Simulating the hydrological response of a small tropical forest watershed (Mata
777 Atlantica, Brazil) by the AnnAGNPS model. Science of the Total Environment 636, 737-750.